

## Experimental investigations on detecting lateral buckling for subsea pipelines with distributed fiber optic sensors

Xin Feng<sup>a</sup>, Wenjing Wu<sup>b</sup>, Xingyu Li<sup>c</sup>, Xiaowei Zhang<sup>d</sup> and Jing Zhou<sup>\*</sup>

*State Key Laboratory of Coastal and Offshore Engineering, Faculty of Infrastructure Engineering,  
Dalian University of Technology, Dalian 116023, China*

*(Received March 31, 2014, Revised January 13, 2015, Accepted January 16, 2015)*

**Abstract.** A methodology based on distributed fiber optic sensors is proposed to detect the lateral buckling for subsea pipelines in this study. Uncontrolled buckling may lead to serious consequences for the structural integrity of a pipeline. A simple solution to this problem is to control the formation of lateral buckles among the pipeline. This firms the importance of monitoring the occurrence and evolution of pipeline buckling during the installation stage and long-term service cycle. This study reports the experimental investigations on a method for distributed detection of lateral buckling in subsea pipelines with Brillouin fiber optic sensor. The sensing scheme possesses the capability for monitoring the pipeline over the entire structure. The longitudinal strains are monitored by mounting the Brillouin optical time domain analysis (BOTDA) distributed sensors on the outer surface of the pipeline. Then the bending-induced strain is extracted to detect the occurrence and evolution of lateral buckling. Feasibility of the method was validated by using an experimental program on a small scale model pipe. The results demonstrate that the proposed approach is able to detect, in a distributed manner, the onset and progress of lateral buckling in pipelines. The methodology developed in this study provides a promising tool for assessing the structural integrity of subsea pipelines.

**Keywords:** subsea pipeline; lateral buckling; buckling detection; structural integrity; distributed fiber optic sensor; BOTDA

### 1. Introduction

With the rapid development of the subsea oil and gas exploitation, more and more pipelines have been built for oil and gas transport. Especially for the deep sea oilfield, subsea pipelines are the arteries of the platforms and floating production systems (Palmer and King 2007). Because these pipelines are laid in deep water there is no requirement for pipeline trenching and therefore no lateral or uplift restraint acting on the pipeline to prevent buckling. Hot oil begins to flow

---

\*Corresponding author, Professor, E-mail: [zhouj@dlut.edu.cn](mailto:zhouj@dlut.edu.cn)

<sup>a</sup> Professor, E-mail: [fengxin@dlut.edu.cn](mailto:fengxin@dlut.edu.cn)

<sup>b</sup> Ph.D. Student, E-mail: [wwjzsl87@126.com](mailto:wwjzsl87@126.com)

<sup>c</sup> Master Student, E-mail: [88725013@163.com](mailto:88725013@163.com)

<sup>d</sup> Master Student, E-mail: [345119997@qq.com](mailto:345119997@qq.com)

The first two authors have the equal contribution to the paper.

through it. Both the rise in temperature and internal pressure lead to longitudinal expansion of the pipeline. The friction between the interface of seabed and pipeline acts to restrain this expansion which results in long-range longitudinal compressive stress in the pipeline. When such compressive stress reaches a critical value, the pipeline buckles laterally into a snake-like profile since it is easier for the pipeline to move sideways on a flat seabed. The buckles sometimes occur with disconcerting suddenness. They have to be taken seriously because they can overstress the pipe wall, occasionally lead to a rupture (Talor and Tran 1996, Miles and Calladine 1999, Karampour *et al.* 2013). A good solution is to manage lateral buckling in a control manner, by deliberately initiating the lateral movement of the pipeline. No matter how to initiate the lateral buckling, monitoring the occurrence and development of the buckles plays an important role for keeping the structural safety of the pipelines.

Lateral buckling is a global structural behavior and often occurs at arbitrary positions over a substantial distance on the pipeline path. The limitation for the discrete sensors is that they can only measure the limited section of the structure instead of covering the full length. Clearly there is a need for a technique that allows strain measurements over lengths of the pipelines. Recent developments of distributed fiber optic sensors based on the Brillouin back-scattering effect provide a promising and cost-effective tool that can monitor the strain and temperature over kilometeric distances. Brillouin based fiber-optic sensors have been used in a number of applications, including monitoring of civil, mechanical, and aerospace structures (Ansari 2007, Bao 2009, Wright 2010, Lee and Sohn 2012, Mohamad *et al.* 2012, Feng *et al.* 2013, Feng *et al.* 2014, Sun *et al.* 2014). For buried and subsea pipelines, Brillouin sensors can meet the requirement of long distance monitoring in a real distributed nature. Zou *et al.* (2004) presented a Brillouin sensor based method to detect the wall-thinning defects in steel pipe under internal pressure. The distributed sensors were installed on the outer surface of the pipe for measuring the axial and hoop strains. Experimental results indicate that the locations of structural indentations that constitute 50-60% of the inner pipe wall are found and distinguished by use of their corresponding strain-pressure data. Ravet *et al.* (2006) proposed a distributed Brillouin sensor based approach to detect the local buckling caused by the wall thinning of the pipe. They conducted the lab experiments to monitor the axial strains of steel pipe under compressive loads using a distributed sensor system. A small peak in the spectrum, corresponds to the elongation of a short length element in the neighborhood of the thinned wall, was extracted as the local buckling feature. Eisler *et al.* (2008) presented a distributed fiber optics temperature system to monitor the pipeline operational conditions and to achieve efficient flow assurance monitoring. The system is used to monitor two offshore pipelines, with 14 km distance in total, in the Alaska's Beaufort Sea Oil field. Nikles (2009) reported a Brillouin based system to detect the pipeline leakage, intrusion and ground movement for pipeline integrity monitoring. The system is capable of measuring strain and temperature over 100's kilometers with meter spatial resolution. Inaudi and Glisic (2010) presented the on-site applications of a distributed sensing system for monitoring the long-range pipelines. They demonstrated the long-range monitoring capability of the system on a 55 km brine pipeline in Berlin. Frings and Walk (2011) used the various physical effects of fiber optic sensors to detect the temperature, strain, vibration and sound for monitoring the structural integrity, third party activities and intrusion over the pipeline. Glisic and Yao (2012) developed a method for buried pipeline health assessment based on distributed fiber optic sensors. The validation of the method was made through a large-scale testing to simulate the structural responses of buried pipeline under the permanent ground displacement. According to the literature survey, the most of the existing approaches use the distributed temperature to detect the leakage of the pipelines. The

temperature based techniques cannot monitor the deformations of the pipelines. The strain based approaches have been adopted to monitor the local damages in the pipelines (Zou *et al.* 2004, Ravet *et al.* 2006, Glisic and Yao, 2012). However, the distributed fiber optic sensors are rarely used to monitor the global buckling of pipelines.

The objective for the work presented in this article was to propose a methodology to detect the lateral buckling for subsea pipeline with distributed fiber optic sensors. The detecting scheme was theoretically formulated by the buckling analysis for the pipelines under the operational loads. Feasibility of the proposed approach was investigated through an experimental program. A model pipe was subjected to the axial compressive force, under different load cases, to drive the lateral buckling. The distributed fiber optic sensors were placed to monitor the longitudinal strains along the pipe. The buckling process and location were then detected by the distributed strains. The results were presented and discussed in this article. The novelty of this study is that the bending-induced strain is used to identify the lateral buckling in the pipe. The sensing scheme of the distributed sensors was proposed and the algorithm to extract the bending-induced strain was presented in the paper.

## 2. Detecting scheme

### 2.1 Theoretical formulation

A pipeline is a slender hollow structure that travels long distance, the hydrocarbon contents in the pipeline usually are at high temperature (80 °C or higher) and high internal pressure (10 MPa or higher). Both the increase in temperature and internal pressure result in longitudinal expansion of the pipeline. The seabed friction acts to restrain this expansion which results in the accumulation of compression stress in the pipe wall that will lead to the buckling. A pipeline lying on the flat seabed will laterally buckle in the horizontal plane while a trenched pipeline will undergo upheaval buckling in the vertical plane. The axial compression force in the pipeline due to restrained longitudinal expansion is given by

$$P = EA\alpha\Delta T_e \quad (1)$$

where  $P$  is the axial compressive force;  $E$  is the Young's modulus of the pipeline;  $A$  is the cross-sectional area of the pipe; and  $\alpha$  is the thermal expansion coefficient of pipe material.  $\Delta T_e$  denotes the combined effects of temperature and internal pressure, which is determined by

$$\Delta T_e = \Delta T + \frac{\rho D(1-2\nu)}{4tE\alpha} \quad (2)$$

where  $\Delta T$  is the variation in the temperature;  $\rho$  is the mass density of the internal hydrocarbon; and  $t$  and  $\nu$  are the wall thickness and Poisson's ratio of the pipe, respectively.

According to the classic theory (Hobbs 1984), the governing equation of the pipeline under the axial compressive force can be expressed as

$$EI \frac{d^2w}{dx^2} + Pw + \frac{\phi q(4x^2-L)}{8} = 0 \quad (3)$$

where  $x$  is the axial position along the pipeline;  $w$  is the lateral displacement;  $I$  is the inertial moment of the cross section of the pipe;  $\phi$  is the frictional coefficient between the pipeline and

the seabed;  $q$  is the intensity of lateral frictional force; and  $L$  is the effective length of the buckle. The schematic illustrations of loading effect and first mode lateral buckling are shown in Fig. 1, and the coordinate system is defined in this figure. In this model, the axial friction is neglected due to that the lateral buckling bifurcation is totally controlled by the lateral resistance. Moreover, Eq. (3) suffers from an assumption that the bending moments are zero at both ends of the buckle.

Based on the above equation, the relationship between axial buckling force,  $P_{cr}$ , and maximum lateral displacement,  $w_m$ , is given by

$$P_{cr} = 3.962 \sqrt{\frac{EI\phi q}{w_m}} \quad (4)$$

When axial compressive force increases, buckling will change to the higher modes. For real subsea pipelines, critical buckling force is less than the values calculated by Eq. (4) because pipelines inevitably have the initial imperfection.

Within the buckle, the pipe is subjected to the combination of axial compressive force and lateral bending moment. The bending moment is caused by the axial compressive force as well as the lateral frictional force. Then the longitudinal strain,  $\varepsilon_L$ , along the pipe can be expressed as

$$\varepsilon_L = \frac{P}{EA} + \frac{MD\sin\theta}{2EI} \quad (5)$$

where  $D$  and  $A$  represent the outer diameter and cross-sectional area of the pipe, respectively; and  $\theta$  is the angle between the arbitrary point on the pipe surface and the neutral axis of the pipe, with the anti-clockwise direction in the cross section (shown in Fig. 1(b)). In the case of lateral buckling, the neutral plane of the pipe is vertical to the seabed.

Eq. (5) is very easily to interpret, where the strain is decomposed into compression-induced strain and bending-induced strain. Thus, for any longitudinal strain on the outer surface of the pipe, Eq. (5) can be rewritten in a compact form.

$$\varepsilon_L = \varepsilon_{comp} + \varepsilon_{bend} \quad (6)$$

where  $\varepsilon_{comp}$  and  $\varepsilon_{bend}$  correspond to the compression-induced strain and bending-induced strain, respectively. Since Eq. (6) has two unknowns, in principle two measured strains at any arbitrary cross section are required to determine them. For simplicity, two distributed fiber optic sensors are placed oppositely with  $\theta = \pi/2$  and  $\theta = 3\pi/2$ , and then the compression-induced strain and bending-induced strain can be obtained.

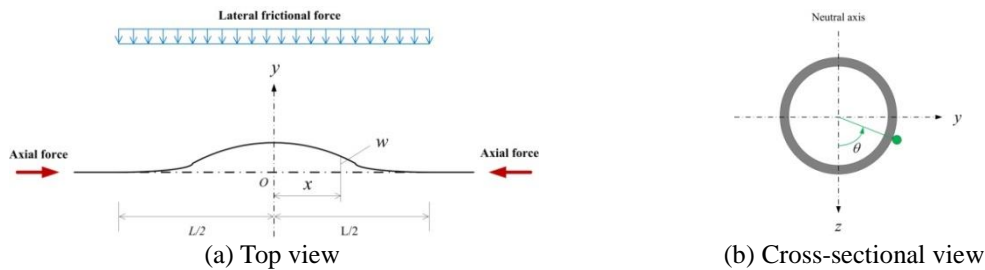


Fig. 1 Schematic illustrations of loading effect and first mode lateral buckling

As previously mentioned, the bending moments at the both ends of the buckle become zero. Thus the position on the pipe where the strain,  $\varepsilon_{\text{bend}}$ , is about zero can be extracted as the feature to identify the start-stop points of the buckle. In this study, the distributions of bending-induced strains derived from Eq. (6) are adopted to detect the occurrence of buckling, while the zero crossing points of the bending-induced strains are used to identify the buckle length and its evolution.

## 2.2 Distributed sensing scheme for buckling detection

Distributed fiber optic sensors consist of a single optical fiber sensitive over its entire length, which is suitable to apply to the pipelines. One of the most applicable approaches for distributed optical fiber sensing is based on Brillouin back-scattering effect. Sensing of strain and/or temperature is achieved by measuring the peak frequency shift (Brillouin shift). The Brillouin shift in optic fiber is the result of interaction of light with phonons, and it is linearly dependent on strain and temperature. Brillouin based sensing approaches use the entire length of the optical fiber for both signal transmission and sensing purpose, and then a distributed sensing with a large monitoring is realized. Various approaches have been used in Brillouin based sensing. The prevalent approaches have been categorized into spontaneous scattering and stimulated scattering based techniques. Brillouin optical time domain reflectometry (BOTDR) is based on the spontaneous technique, whereas Brillouin optical time domain analysis (BOTDA) employs the stimulated scattering technique. By comparing with former one, BOTDA can reach higher spatial resolution and measurement accuracy. For this reason BOTDA system was adopted in this study.

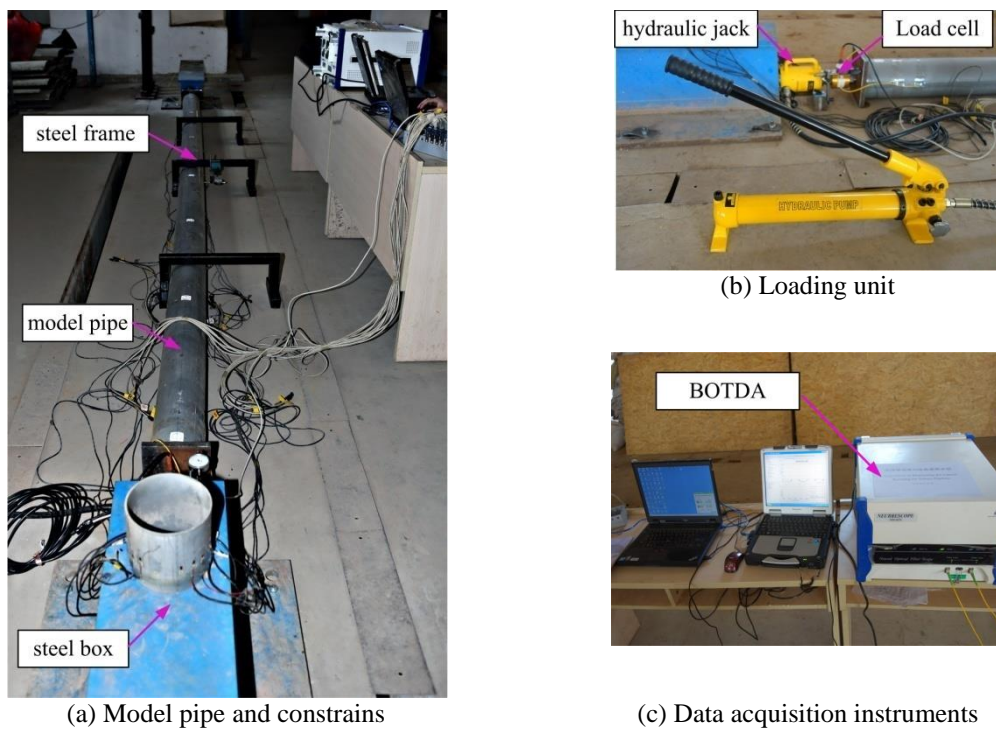


Fig. 2 Experimental setup

The capability of distributed fiber optic sensors to reliably monitor the lateral buckling depends on their topology, and more specifically, on their positions on the pipeline. Based on the previous analysis, to obtain the compression-induced and bending-induced strains, two sensors at  $\theta = \pi/2$  and  $\theta = 3\pi/2$  in the cross section (defined as Fig. 1(b)) were selected for monitoring. Thus the sensing fiber can be a loop on the monitored pipeline. In this system, BOTDA instrument is employed to interrogate the distributed strains in the sensing fibers. Once the measured strains were obtained, the compression-induced and bending-induced strains can be derived by Eq. (6), and then the buckling of the pipe can be detected by using the distributions of bending-induced strains. The detection results of lateral buckling will be reported to the owner for safety assessment and operation decision-making.

### 3. Experimental setup

We conducted a series of model tests to evaluate the feasibility of the proposed methodology. The experimental program involved use of the BOTDA sensor system for distributed measurement of strain and detection the lateral buckling of the model pipe. The main purpose of the present study is to investigate the performance of the detection method with the distributed sensor, instead of the structural behavior of the prototype pipeline. Hence the similitude between model and prototype was not considered in the experiments.

The model is a polyvinyl chloride (PVC) pipe with the length of 5.47 m. The outer diameter of the pipe is 160 mm, and the wall thickness is 5 mm. The Young's modulus of the pipe is 13.77 GPa.

The experiment apparatus was designed to simulate the lateral buckling of pipeline under axial compression. The experimental setup, shown in Fig. 2, consists of three units: loading unit, constrain unit, and instrumentation unit. Two steel boxes were fixed on the base with expansion anchor bolts, which provide constrains on the model pipe and loading unit. Two steel plates with 10 mm thickness were used to fix the model pipe between the right steel box and loading unit. A 5 mm deep circle groove, with the same diameter as the pipe, was dug out of each steel plates. Then the model pipe was inserted into the steel plates at both ends. The 2 mm thickness elastic gaskets inside the grooves were used to provide the cushions for the pipe. A hydraulic jack was placed between the left steel box and the pipe for axially compressing the model pipe. Three steel frames were anchored in the even space to keep the pipe closely on the base. Meanwhile, the frames were used to prevent the upheaval buckling of the pipe. Since the pipe fits the base well, the lateral as well as axial frictions are created when axial force is applied.

A commercially available telecommunication type single mode optical fiber, Corning SMF-28, was adopted as the distributed sensor. The optical fiber was pre-tensioned and then adhered by epoxy resin to the outer surface of model pipe, with  $\theta = \pi/2$  and  $\theta = 3\pi/2$ , along the entire length of the pipe. The sensing fiber forms a loop. The segment of sensing fiber corresponding to  $\theta = \pi/2$  is designated as Sensor 1, whereas another segment is named as Sensor 2. The sensor locations of Brillouin sensors are shown in Fig. 3(a). The distributed strains were measured by a BOTDA interrogator NBX-6050A (Neubrex, Japan). For each load cases, three different spatial resolutions, i.e., 10 cm, 20 cm, and 50 cm, were selected to perform the measurements. In this article, only the results of 10 cm spatial resolution are presented since they can provide more accurate data. The distance resolution, i.e. sampling interval, is 5 cm in all measurements. Hence the really distributed sensing achieves.

Table 1 Load cases for axial compressive force performed on model pipe

Load case	1	2	3	4	5	6
Axial force (kN)	5.50	11.50	19.80	24.60	28.10	42.30

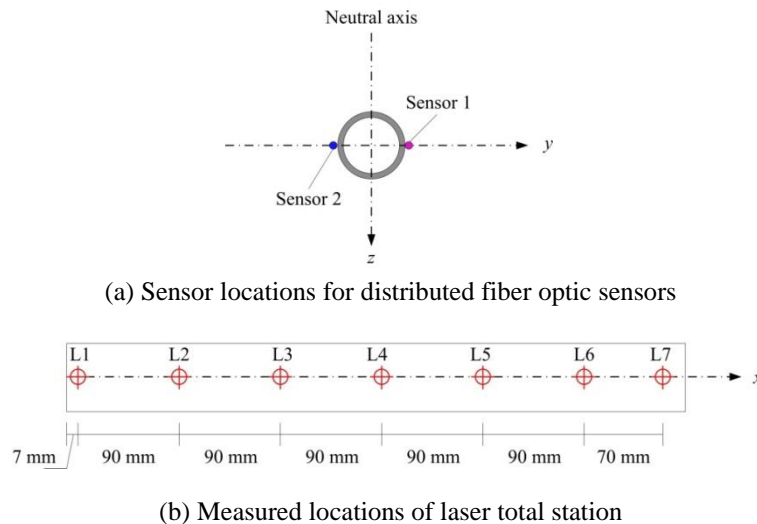


Fig. 3 Schematic illustrations for measured locations

It was necessary to independently monitor the deformations of model pipe. A laser total station RTS 311L, manufactured by FOIF Inc., China, was used to measure the lateral and axial displacements on the neutral axis of model pipe for each load cases. The measured locations are illustrated in Fig. 3(b). The laser total station possesses high accuracy of deformation measurement with 1/10 mm.

The lateral buckling of model pipe is driven by the axial compression, and thus the axial force applied by the hydraulic jack should be monitored. A load cell was employed to measure the axial force. The load cell is the full bridge transducer. The measurements were collected by NI compact DAQ. Six load cases, in total, were considered for testing the occurrence and evolution of the lateral buckling. Each axial compressive force for six load cases is shown in Table 1.

#### 4. Experimental results and analysis

The axial compressive force was applied by the hydraulic jack. In this study, the initial shape of the model pipe was not deliberately set because the model pipe is not an ideal straight pipe. The initial imperfection of the pipe, in the shape of small arch, can be found by the naked eyes with amplitude of several millimeters. Thus we placed the pipe in the direction that it is easier to drive the lateral buckling. For each load cases, the longitudinal strains were measured by the distributed fiber optic sensors. The distributed strains from two sensors (i.e., Sensor 1 and Sensor 2) are plotted in Fig. 4 for total six load cases, while the lateral displacements of the pipe are shown in

Fig. 5. For load case 1, the lateral displacements are very small but the longitudinal strains are not constant. It is indicated that the model pipe was subjected to bending moments even in small axial compression, which are caused by the initial imperfection of the pipe shape. In this load case, all the measured strains are negative and the measurements of Sensor 1 and Sensor 2 are intersected at 1.35 m and 2.95 m. With the increase of the axial force, the lateral displacements of model pipe become larger and larger, and the bending behavior appears more and more obvious. Meanwhile, the longitudinal strains of Sensor 1 tend to tensile strains with increasing amplitude, whereas the measurements of Sensor 2 approach to the larger and larger negative values. In Fig. 4, the maximum longitudinal strain of load case 6 is much greater than the yield strain of model pipe (i.e.,  $\epsilon_y = 2900 \mu\epsilon$ ), while the lateral displacements suddenly increase with the respect to the first five load case. In the last load case, one small fracture was observed in the pipe during applying the load, which indicates that the pipe has reached the failure phase. On the whole, the measured longitudinal strains by the distributed sensors can reveal the bending behavior of the model pipe; however, they cannot be used to detect the occurrence and evolution of the lateral buckling. Therefore, the further analysis should be performed on the measured data.

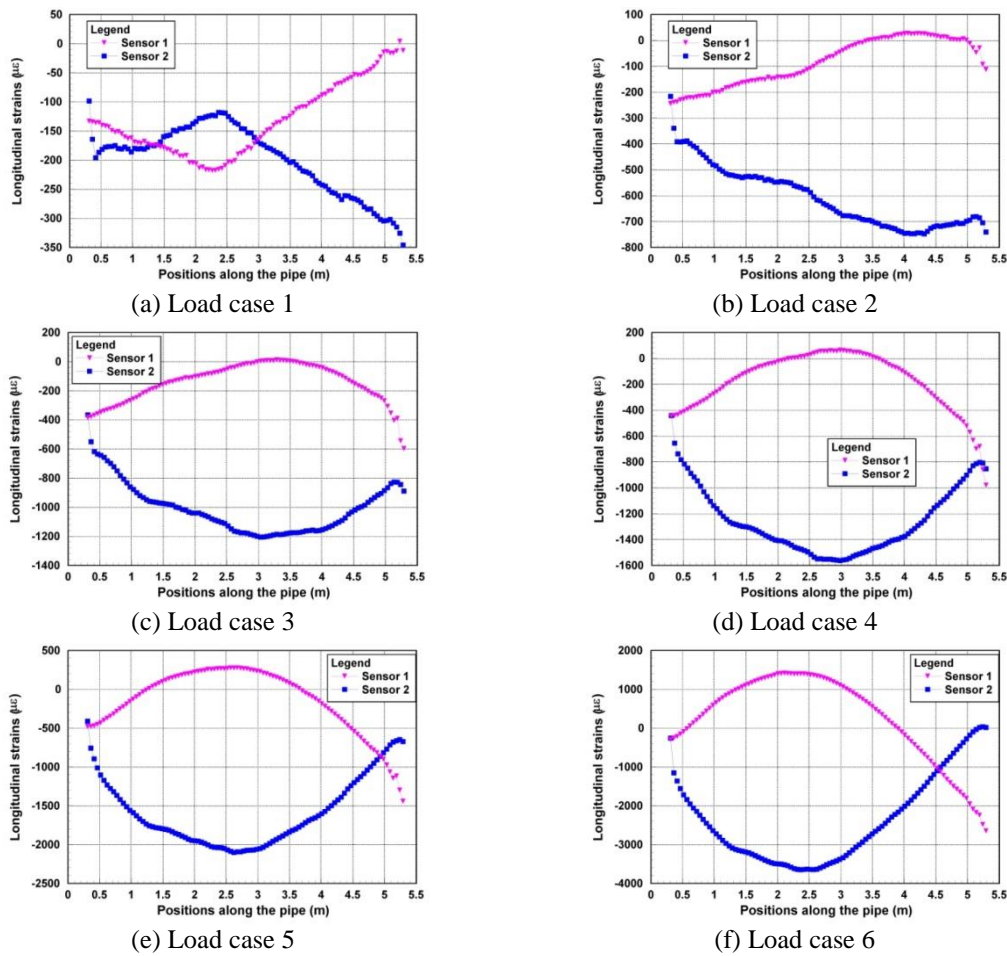


Fig. 4 Distributed measurements of longitudinal strains

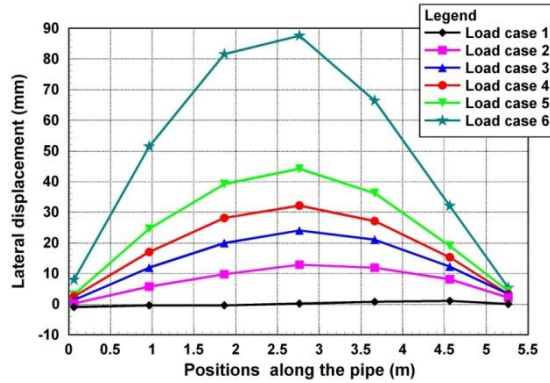


Fig. 5 Measured lateral displacement for six load cases

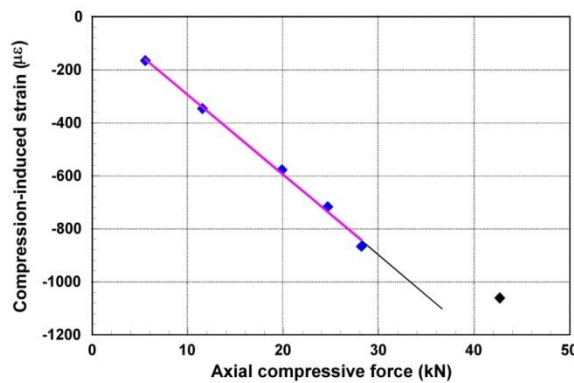


Fig. 6 Relationship between compression-induced strains and axial force

Based on Eq. (6), the compression-induced strain and bending-induced strain are extracted from the measurements of two distributed sensors. For each load cases, the mean values of the compression-induced strains were calculated, and the relationship between them and axial compressive force is shown in Fig. 6. The isolated point in the figure corresponds to the last load case. It clearly demonstrates that the compression strains linearly correlate to the axial force for the first five load cases. But for load case 6, the compression-induced strain deviates from the linear relationship, which means that the pipe has entered its failure phase.

The calculated compression-induced and bending-induced strains are plotted in Figs. 7-12. The figures clearly demonstrate the progress on lateral buckling of model pipe. For load case 1, by using the detecting principle stated in Section 2, a small buckling lobe can be identified according to two zero-crossing points at 1.35 m to 2.95 m. Within the buckling lobe, the bending-induced strains measured by Sensor 1 are the compressive strains, whereas those measured by Sensor 2 are the tensile strains. This phenomenon is caused by the lateral deformation of buckling lobe is towards to the negative direction of y-axis (defined in Fig. 1), which agrees with the measured lateral displacements in Fig. 5.

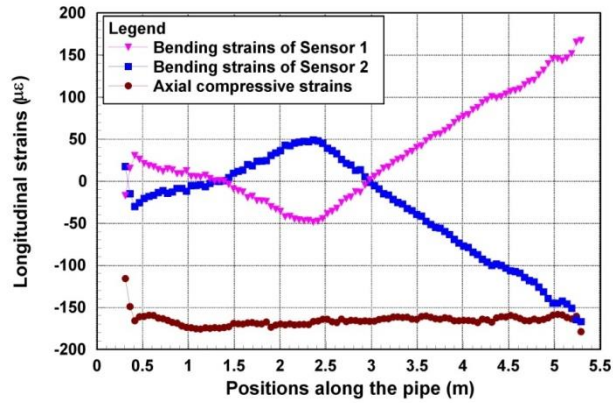


Fig. 7 Compression-induced strains and bending-induced strains for load case 1

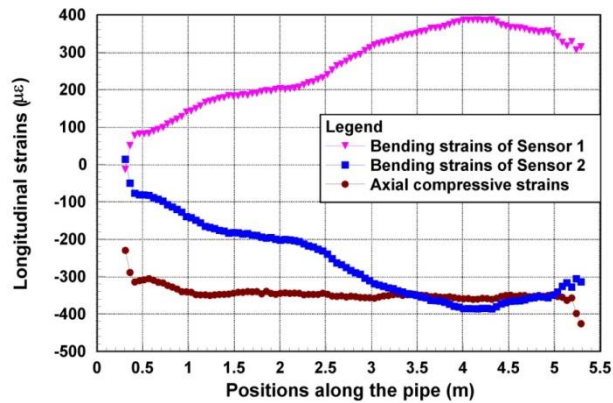


Fig. 8 Compression-induced strains and bending-induced strains for load case 2

In Figs. 8-10, the buckling lobe is extinct with the increase of the axial force. Although the axial compressive force becomes larger, the lateral displacements of model pipe are in the positive direction of  $y$ -axis. And hence the bending effect that drives the first buckling lobe disappeared in this stage. All the axial compressive force only provides the driven force for the lateral buckling in the opposite to the small buckling lobe. Up to load case 4, the drive force is large enough to form a global lateral buckling on the model pipe. In Fig. 10, two zero-crossing points can be clearly found. In a result, the global lateral buckling can be detected by this phenomenon. Based on buckling theory of pipe, we know that this buckle is the first global mode of lateral buckling. From Section 2.1, the critical buckling force of the test pipe should be 33.20 kN in the case that the pipe is perfect straight. In our experiments, however, the test pipe has the initial imperfection which results in the reduction of the buckling force. The axial force for load case 4 is measured as 24.60 kN which corresponds to the first mode buckling of the test pipe. It is demonstrated that the actual buckling force is much less than the calculated force for the straight pipe.

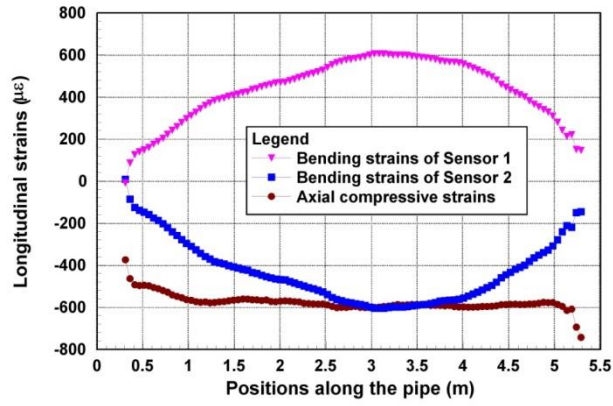


Fig. 9 Compression-induced strains and bending-induced strains for load case 3

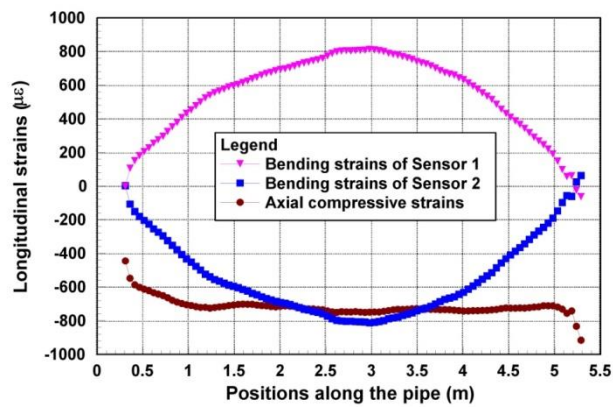


Fig. 10 Compression-induced strains and bending-induced strains for load case 4

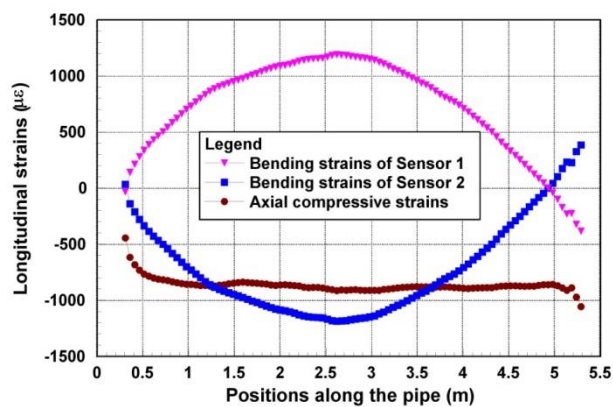


Fig. 11 Compression-induced strains and bending-induced strains for load case 5

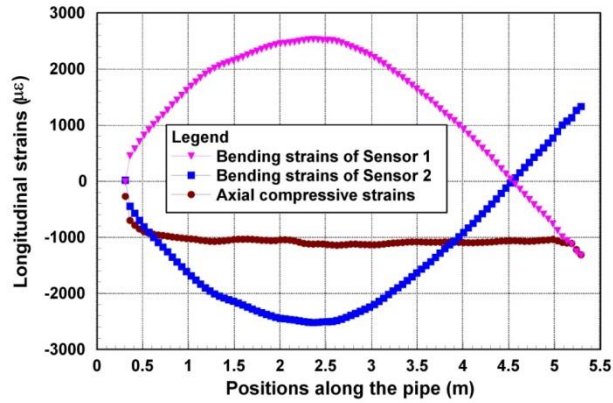


Fig. 12 Compression-induced strains and bending-induced strains for load case 6

From Fig. 11, it can be seen that the length of the first mode buckling narrows due to the growing of axial force. The neighbor region, corresponding to the higher buckling modes, is actuated with continuously increasing length. For the last load case, the bending-induced strains increase further, and the buckling length become narrower (shown in Fig. 12). By comparing with the first four load cases, the increase of compression-induced strain significantly falls behind the growing of bending-induced strains. It indicates that the bending effect is more active to form a new buckle. In these two load cases, the bending deformation close to the right end of model pipe has the opposite direction to the other parts. This behavior agrees with the observations, from Fig. 5, that the lateral displacement in location L6 is less than that in location L2. If the axial force is larger enough, the second mode of lateral buckling will occur. Since the fracture happen in load case 6, we didn't continuously apply the load. However, according to the observations of whole experimental progress, it should be pointed out that the proposed method can detect both the pre-buckling and post-buckling behavior of the pipelines. For real engineering, the evolution of lateral buckling must be treated with some caution, not only in regard to the ultimate limit state of subsea pipeline, but also with respect to validate the design of controlling and initiating the buckling.

## 5. Conclusions

The work presented in this article pertained to the development of a methodology for detecting the lateral buckling of subsea pipelines with distributed fiber optic sensors. Uncontrolled buckling can have serious consequences for the structural integrity of a pipeline. The cost-effective solution to this problem is to work with rather than against the pipeline by controlling the formation of lateral buckles among the pipeline. This firms the importance of monitoring the pre-buckling and post-buckling behavior of pipelines during the first months and years after start-up. The results of buckling detection can be used to assess the ultimate limit state, check buckle formation reliability, determine peak loads and cyclic stresses in buckles, and validate the pipeline design. The present work involved in using distributed sensor to monitor the evolution of lateral buckling for subsea pipelines. The primary advantage in using the Brillouin based fiber optics sensor is their

distributed sensing capacity over the entire length of pipeline. This study included determination of sensing scheme and feasibility validation by a small-scale experiment. The lateral buckling was simulated by applying the axial compressive loads on a 5.47 m long model pipe. A BOTDA system was employed for distributed measurement of longitudinal strains and detection of lateral buckling. The distributions of bending-induced strains, derived from the measured longitudinal strains, were used to identify the occurrence and evolution of buckles. For load case 1, a small buckling lobe due to the initial imperfection was detected in the experiment. With the increase of the load, the buckling lobe disappeared and the growing axial compressive force tends to form new buckle in the pipe. Up to load case 4, a first mode buckling was detected by the distributed sensors when the axial force reaches the critical buckling load. After that, the evolution of lateral buckling was detected with that the length of first mode buckling becomes smaller. The distribution of bending-induced strains indicates that the second mode buckling will occur. For load case 6, the measured strain is greater than the yield strain of model material and fracture happened on the pipe. And hence the measured strain can be adopted to assess the ultimate limit state of pipeline, except for monitoring the evolution of buckling. In summary, the results of this study indicate that it is possible to detect the occurrence and evolution of lateral buckling in subsea pipelines with distributed fiber optic sensors. It should be noted that the present study only demonstrates the feasibility of the proposed sensing scheme by the lab scale experiments. In real applications, the relative locations between sensors and seabed may be distorted in some cases. The effects of the undesired sensor setup may lead to the errors of the monitored data. Thus the more robust sensing scheme and the powerful signal processing approaches should be studied in the future to enhance the capability of the proposed method. Moreover, further research is also necessary to examine the performance of the approach under real ocean environment and complex buckling pattern, for example, the combination mode of lateral and upheaval buckling.

## Acknowledgments

This research is based on work supported by the State Key Development Program for Basic research of China (No. 2011CB013702), and grants from the National Natural Science Foundation of China under Grant No. 51421064 and 51378088 as well as from the Fundamental Research Funds for the Central Universities (No. DUT14ZD202). We are grateful to Prof. Yongbo Yuan and PhD student, Chenlong Liu, for providing the deformation monitoring with laser total station.

## References

- Ansari, F. (2007), "Practical implementation of optical fiber sensors in civil structural health monitoring", *J. Intel. Mat. Syst. Str.*, **18**(8), 879-889.
- Bao, X. (2009), "Optical fiber sensors based on Brillouin scattering", *Optics Photonics News*, **20**(9), 40-46.
- Eisler, B., Lanan, G., Nikles, M. and Zuckerman, L. (2008), "Distributed fiber optic temperature sensing system for buried subsea arctic pipelines," *Proceedings of the Deep Offshore Technology International Conference & Exhibition – DOT'08*, Houston, USA.
- Feng, X., Zhou, J., Sun, C., Zhang, X. and Ansari, F. (2013), "Theoretical and experimental investigations into crack detection with BOTDR-distributed fiber optic sensors", *J. Eng. Mech. - ASCE*, **139**(12), 1797-1807.
- Feng, X., Zhang, X., Sun, C., Motamedi, M.H. and Ansari, F. (2014), "Stationary wavelet transform method

- for distributed detection of damage by fiber-optic sensors”, *J. Eng. Mech. - ASCE*, **140**(4), 1-11.
- Frings, J. and Walk, T. (2011), “Distributed fiber optic sensing enhances pipeline safety and security”, *Oil Gas Eur. Mag.*, **2**, 132-136.
- Glisic, Y. and Yao, Y. (2012), “Fiber optic method for health assessment of pipelines subjected to earthquake-induced ground movement”, *Struct. Health Monit.*, **11**(6), 696-711.
- Hobbs, R.E. (1984), “In-service buckling of heated pipelines”, *J. Transport. Eng.*, **110**(2), 175-189.
- Inaudi, D. and Glisic, B. (2010), “Long-range pipeline monitoring by distributed fiber optic sensing”, *J. Pressure Vessel Technol.*, **132**(1), 011701-1-9.
- Karampour, H., Albermani, F. and Gross J. (2013), “On lateral and upheaval buckling of subsea pipelines”, *Eng. Struct.*, **52**, 317-330.
- Lee, H. and Sohn, H. (2012), “Damage detection for pipeline structures using optic-based active sensing”, *Smart Struct. Syst.*, **9**(5), 461-472.
- Miles, D.J. and Calladine, C.R. (1999), “Lateral thermal buckling of pipelines on the sea bed”, *J. Appl. Mech. - T ASME*, **66**(12), 891-897.
- Mohamad, H., Soga, K., Bennett, P., Mair, R.J. and Lim, C.S. (2012), “Monitoring twin tunnel interaction using distributed optical fiber strain measurements”, *J. Geotech. Environ. Eng.*, **138**(8), 957-967.
- Nikles, M. (2009), “Long-distance fiber optic sensing solutions for pipeline leakage, intrusion and ground movement detection”, *Proceedings of SPIE*, **7316**(2), 1-13.
- Palmer, A.C. and King, R.A. (2007), *Subsea pipeline engineering*, (2nd Ed.), PennWell, Oklahoma, USA.
- Ravet, F., Zou, L., Bao, X., Chen, L., Huang, R.F. and Khoo, H.A. (2006), “Detection of buckling in steel pipeline and column by the distributed Brillouin sensor”, *Opt. Fiber Technol.*, **12**(4), 305-311.
- Sun, Y., Shi, B., Chen, S., Zhu, H., Zhang, D. and Lu, Y. (2014), “Feasibility study on corrosion monitoring of a concrete column with central rebar using BOTDR”, *Smart Struct. Syst.*, **13**(1), 41-53.
- Taylor, N. and Tran, V. (1996), “Experimental and theoretical studies in subsea pipeline buckling”, *Marine Struct.*, **9**(2), 211-257.
- Wright, P. (2010), “Assessment of London underground tube tunnels - investigation, monitoring and analysis”, *Smart Struct. Syst.*, **6**(3), 239-262.
- Zou, L., Ferrier, G.A., V. Afshar, S., Yu, Q., Chen, L. and Bao, X. (2004), “Distributed Brillouin scattering sensor for discrimination of wall-thinning defects in steel pipe under internal pressure”, *Appl. Optics*, **43**(7), 1583-1588.